



## Pool boiling heat transfer on copper foam covers with water as working fluid

Yongping Yang, Xianbing Ji, Jinliang Xu\*

Beijing Key Laboratory of New and Renewable Energy, North China Electric Power University, Beijing 102206, PR China

### ARTICLE INFO

#### Article history:

Received 26 July 2009

Received in revised form

23 December 2009

Accepted 12 January 2010

Available online 12 February 2010

#### Keywords:

Copper foam

Pool boiling

Boiling curve

### ABSTRACT

Pool boiling heat transfer with porous media as the enhanced structure is attractive due to its simple geometry and easy operation. However, the available studies focus on low porous porosities. Metallic foams provide large porous porosities that have been less studied in the literature. In this paper a set of copper foam pieces were welded on the plain copper surface to form the copper foam covers for the pool boiling heat transfer enhancement. Water was used as the working fluid. Enhancement of pool boiling heat transfer compared with plain surface depends on the increased bubble nucleation sites, extended heat transfer area, and resistance for vapor release to the pool liquid. Effects of pores per inch (ppi) of foam covers, foam cover thickness, and pool liquid temperatures are examined. It is found that temperatures at the Onset of Nucleate Boiling (ONB) are significantly decreased on copper foam covers compared with on plain surfaces. Heat transfer coefficients of foam covers are two to three times of the plain surface. A large ppi value provides large bubble nucleation sites and heat transfer area to enhance heat transfer, but generates large vapor release resistance to deteriorate heat transfer. Therefore an optimal ppi value exists, which is 60 ppi in this paper. Generally small ppi value needs large foam cover thickness, and large ppi value needs small foam cover thickness, to maximally enhance heat transfer. Effect of pool liquid temperature on the heat transfer enhancement depends on the ppi value. For small ppi value such as 30 ppi, lower pool liquid temperature can dissipate higher heat flux at the same wall superheat. However, the heat transfer performance is insensitive to the pool liquid temperatures when large ppi values such as 90 ppi are used.

© 2010 Elsevier Masson SAS. All rights reserved.

### 1. Introduction

Due to the limitation of the conventional forced convective fan cooling method and increased heat generation of electronic components, reliable cooling methods for electronic devices shall be developed. The required heat removal rate for a CPU is  $6.25 \text{ W/cm}^2$  or more and a printed circuit board produces about  $10 \text{ W/cm}^2$ . In the near future the heat flux of the electronic devices will be more than  $100 \text{ W/cm}^2$ . The widely used fan cooling method using forced convective air as the working fluid, however, is not suitable for high heat fluxes such as larger than  $10 \text{ W/cm}^2$ . Besides, it has problems such as noise, electrical failure, and high power consumption. Therefore, a direct immersion cooling has been suggested as an alternative to the forced convective air cooling methods. Liquids have advantages of higher thermal conductivity, density, and specific heat over air, ensuring high heat flux that is to be dissipated.

Many studies have tried to improve the pool boiling heat transfer by coating a heater surface with a thin, porous layer of particles and reduce the cost and size of equipments. The available studies focus on the boiling heat transfer enhancement using porous media with low porosities.

Bergles and Chyu [1] studied pool boiling heat transfer using a porous structure with a porous porosity of 50–65%, a porous-layer thickness of 0.38 mm, the range of particle sizes of 75% between  $74 \mu\text{m}$  and  $44 \mu\text{m}$ . The result shows that the porous coating can improve boiling heat transfer significantly and decrease the surface superheat.

Rainey and You [2] performed an experimental study of “double enhancement” behavior in pool boiling from heater surfaces simulating microelectronic devices immersed in saturated FC-72 at atmospheric pressure. The term “double enhancement” refers to the combination of two different enhancement structure enhancement techniques: a large-scale area enhancement (square pin fin array) and a small-scale surface enhancement (microporous coating). Results showed significant increases in nucleate boiling heat transfer coefficients with the microporous coating to the heater surface.

Liter and Kaviani [3] demonstrated modulated (periodically non-uniform thickness) porous-layer coatings, as an example of

\* Corresponding author. Tel./fax: +86 10 51976819.

E-mail address: [xjl@ncepu.edu.cn](mailto:xjl@ncepu.edu.cn) (J. Xu).

Nomenclature	
$a_0$ and $a_1$	empirically determined constants for temperature distribution in copper block
$C_{pf}$	specific heat of saturated liquid, kJ/kg K
$C_{pg}$	specific heat of saturated vapor, kJ/kg K
$d_f$	copper ligament diameter, mm
$d_p$	pore diameter of copper foam, mm
$En$	heat transfer enhancement ratio with copper foam to plain surface
$g$	gravity force acceleration, $m\ s^{-2}$
$h$	heat transfer coefficient with foam structure, $W\ m^{-2}\ K^{-1}$
$h_o$	heat transfer coefficient with plain smooth surface, $W\ m^{-2}\ K^{-1}$
$h_{fg}$	latent heat of evaporation, $J\ Kg^{-1}$
$k_s$	thermal conductivity of solid copper, $W\ m^{-1}\ K^{-1}$
$L$	heater surface side length, m
$L_{tran}$	dimensionless surface length
$l$	ligament length of a unit cell, m
$m$	mass flux of vapor phase, $kg\ m^{-2}\ s^{-1}$
$ppi$	the number of pores per inch length of metal foam
$q$	heat flux at the base surface, $W\ m^{-2}$
$q_{CHF}$	critical heat flux, $W\ m^{-2}$
$q_{CHF,small}$	critical heat flux at small heater size, $W\ m^{-2}$
$q_{CHF,large}$	critical heat flux at large heater size, $W\ m^{-2}$
$T$	temperature K or $^{\circ}C$
$V$	volume of a foam cell, $m^3$
$z$	coordinate perpendicular to the base surface, m
$\frac{dT}{dz} _{base\ surface}$	temperature gradient at the base surface, $K\ m^{-1}$
$\delta$	thickness of foam cover, mm
$\Delta T_{sat}$	wall superheat, K or $^{\circ}C$
$\varepsilon$	porosity of foam cover
$\mu$	viscosity, $kg\ m^{-1}\ s^{-1}$
$\rho$	density, $kg\ m^{-3}$
$\sigma$	surface tension force, $N\ m^{-1}$
<b>Subscripts</b>	
bulk	pool bulk condition
f	liquid phase
g	vapor phase
sat	saturation condition
w	wall surface condition

capillary artery-evaporator systems, to enhance the pool boiling critical heat flux nearly three times over that of a plain surface. The modulation separates the liquid and vapor phases, thus reducing the liquid-vapor counterflow resistance adjacent to the surface. Theories are suggested for two independent mechanisms capable of causing the liquid choking that leads to the critical heat flux.

Kim et al. [4] studied the nucleate pool boiling heat transfer enhancement mechanism of microporous surfaces immersed in saturated FC-72. They measured bubble size, frequency, and vapor flow rate from a plain and microporous platinum wire using the consecutive photo technique. It is found that the microporous coatings enhance nucleate boiling performance through increased latent heat transfer in the low heat flux region and through increased convection heat transfer in the high heat flux region.

Ghiu and Joshi [5] conducted visualization study at atmospheric pressure from top covered enhanced structure for a dielectric fluorocarbon liquid (PF 5060). The single layer enhanced structures were fabricated in copper and quartz, having an overall size of 10 mm by 10 mm and 1 mm thick. The heat transfer performance of the enhanced structures was found to depend weakly on the channel width. The internal evaporation has a significant contribution to the total heat dissipation.

Parker and El-Genk [6] studied enhancements in nucleate boiling of FC-72 liquid on porous graphite and compared results with those on a smooth copper surface of the same dimensions (10 mm by 10 mm). Also investigated is the surface temperature excursion at boiling incipience and the obtained values of CHF are compared with those of other investigators. Results showed no temperature excursion at boiling incipience on porous graphite but as much as 14 K on plain copper surface. The heat transfer coefficients are significantly higher than those on copper surface and the values of CHF are 63–94% higher than on copper surface.

Hwang and Kaviany [7] found that the porous surface can enhance the critical heat flux ( $q_{CHF}$ ) and reduce the superheat across the wick in pool boiling.

Recently Min et al. [8] developed a new fabrication method (hot-powder compaction) to make 2-D and 3-D modulated coatings for enhanced pool boiling performance. The results show that the maximum measured critical heat flux ( $q_{CHF}$ ) of 2-D and 3-D

modulated coatings are 3.3 and 2.0 times that of the surface without coatings (plain). The critical heat fluxes strongly depend on the modulation wavelength, while particle diameter and porosity have little effects. The porous porosity of their study is 43.8%.

The above review of the pool boiling heat transfer on porous media surfaces such as porous coatings (particles), porous graphite refers to low porous porosity such as less than 65%. Metallic foam is a new kind of porous media for the heat transfer applications, having large surface to volume ratio and low density. Metallic foam is a structure characterized by thin fibers, or ligaments, of metal joining several others in a random manner throughout the volume. The porous porosity can be larger than 90%. Fewer studies have been reported on the pool boiling heat transfer enhancement with metallic foam structures in the open literature. Several reports on this topic can be found in some conference papers which are shortly described as follows.

Arbelaez et al. [9] reported pool boiling heat transfer of FC-72 in highly porous metal foam heat sinks. The porous porosities were in the range of 90–98% and pore sizes had the range of 5–40 ppi. It is shown that the temperature excursion usually observed for fluorinated fluids at the onset of nucleate boiling is not present. The low porosity samples exhibit a significantly enhanced heat transfer in the low heat flux regions for the same pore size. Enhanced heat transfer is observed with an increase in the foam ppi for similar porosity.

Athreya et al. [10] studied effects of orientation and geometry on the pool boiling heat transfer of FC-72 in high porosity aluminum metal foam heat sinks. It is found that high ppi samples deteriorate heat transfer in the vertical orientation. The low ppi sample first decreases and then increases the heat transfer coefficients with reduction in the foam height.

Moghaddam and Ohadi [11] investigated pool boiling heat transfer of water and FC-72 on thin blocks bonded with copper foams of 80 ppi, 90% porosity, 30 ppi, 95% porosity, and graphite foam of 75% porosity. On the 30 ppi copper foams, significant enhancement was observed in boiling of water. But no enhancement was observed on the 80 ppi copper and graphite foams. A substantial enhancement was achieved on all the foams with FC-72 as the working fluid.

In this paper we study the pool boiling heat transfer on copper foam covers with water as the working fluid. Experiments were performed at atmospheric pressure. Significant heat transfer enhancement is observed. By using copper foam covers temperatures at the ONB can be decreased by 13 K, maximally. Heat transfer coefficients with copper foam cells can be two to three times of those with plain surface, maximally. Bubble nucleation sites, extended heat transfer area and resistance for produced vapor release are the key factors to influence the enhanced heat transfer on copper foam covers. There are optimal ppi values and foam cover thickness to enhance heat transfer, maximally. Coupling of pool liquid temperature and foam cover thickness is observed to influence heat transfer.

## 2. Copper foam parameters

Copper foams for the ppi of 30, 60 and 90 at the porosity of 0.88 are shown in Fig. 1(a–c). Photos of foam covers with the porosity of 0.95 are not given here because they have small difference with those for the porosity of 0.88. Copper foams have open-celled structures composed of dodecahedron-like cells, possessing 12 to 14 pentagonal or hexagonal faces. Porosity and ppi are the two parameters to influence flow and heat transfer. The ligament cross section depends on porosity, and changes from a circle at  $\varepsilon = 0.85$  to an inner concave at  $\varepsilon = 0.97$ , where  $\varepsilon$  is the porosity (Calmidi [12]). A unit cell of the foam is shown in Fig. 1d, with the assumed tetrakaidecahedron shape. The ligament length is  $l$  with its diameter of  $d_f$ . Thus the

volume of a unit cell is  $V = 8\sqrt{2}l^3$ . The circumscribed diameter of the foam cell is  $\sqrt{10}l$ , which can be regarded as the pore diameter of  $d_p$ , i.e.  $d_p = \sqrt{10}l$ , not considering the ligament thickness.

The foam cell parameters were measured by a Leica M-type microscope (Germany) and are given in Table 1. The larger the ppi, the smaller the pore diameter of  $d_p$  and ligament diameter of  $d_f$  are. At the given ppi, larger porosity such as 0.95 leads to slight larger  $d_p$  and smaller  $d_f$ , compared with the lower porosity of 0.88.

## 3. The test section and experimental setup

The geometry and dimensions of the copper block test section are given in Fig. 2a. There are five 6.0 mm diameter holes in which five cartridge heaters were inserted, providing heating power to the copper block, in the bottom part of the copper block. A maximum power of 100 W at the applied AC voltage of 220 V can be provided by each heater. The copper block has a middle part, having three 1.0 mm diameter holes, inside which three K-type thermocouples are inserted. A rectangular plate with a thickness of 3.0 mm is located at the top of the copper block. A plain smooth, sand polished copper surface is regarded as the reference surface for the boiling heat transfer experiment, with the size of 12.0 mm by 12.0 mm. For the pool boiling heat transfer enhancement, the top copper surface was welded with copper foam covers, with five different thicknesses of 1.0, 2.0, 3.0, 4.0 and 5.0 mm, respectively. The copper block was cleaned by methanol and baked in an oven. Then it was taken out of the oven and heated by the cartridge

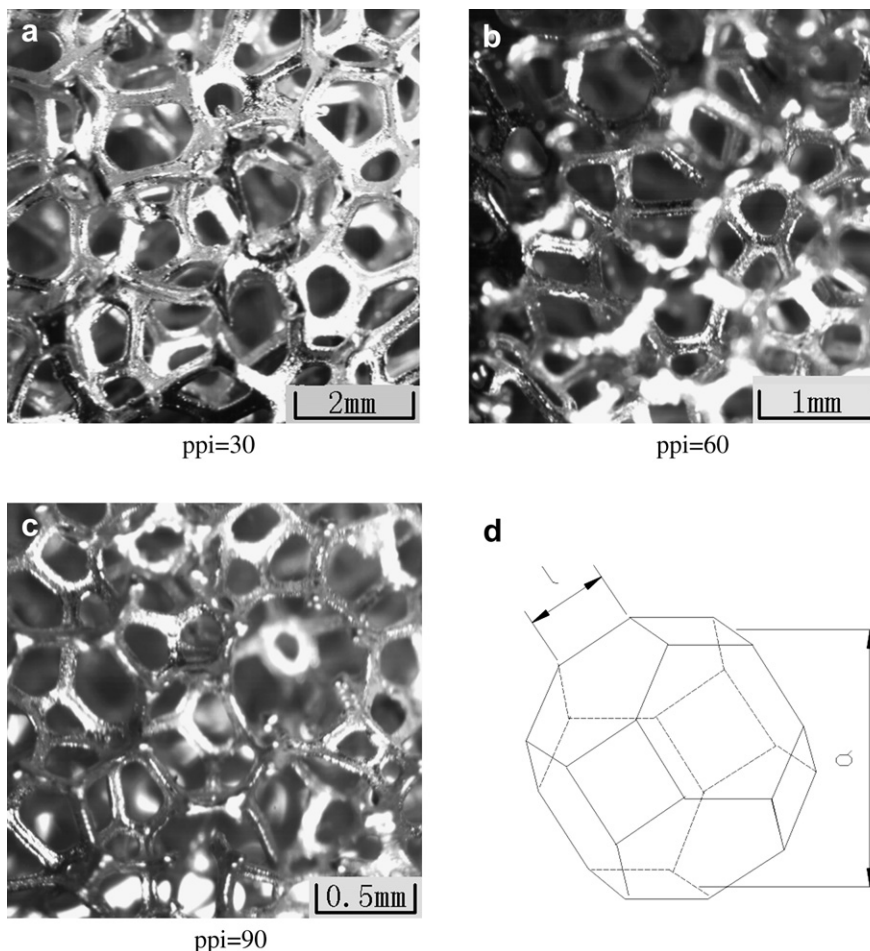
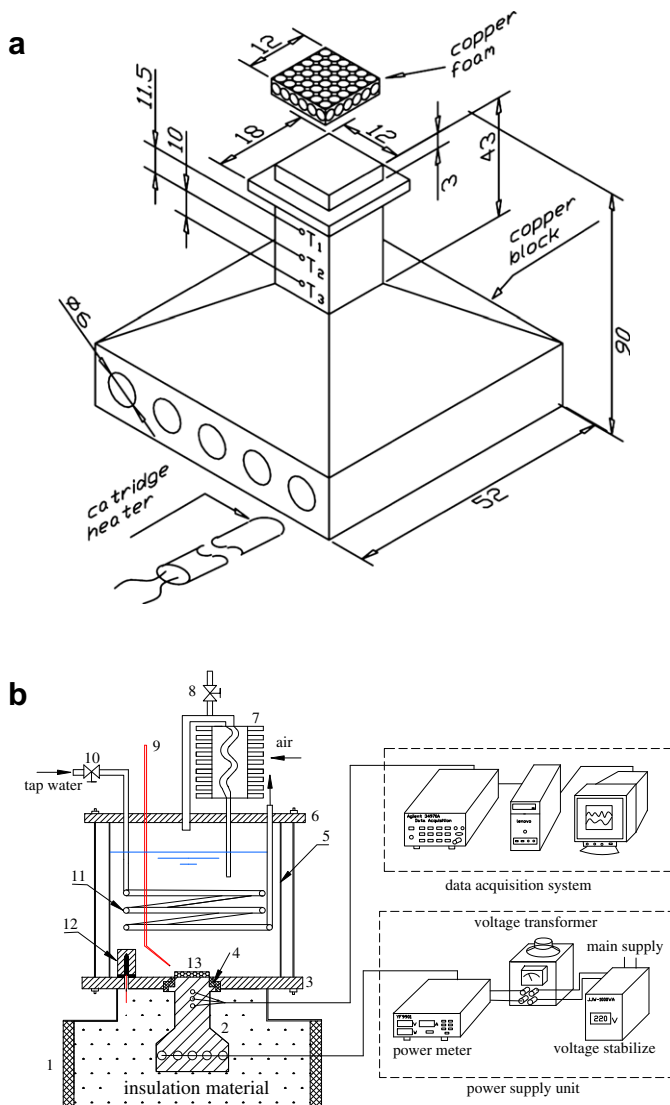


Fig. 1. The copper foam photos for  $\varepsilon = 0.88$  (a, b and c) and a unit foam cell (d).

**Table 1**  
Parameters of the foam cells used in the present paper.

ppi	$\varepsilon$	$d_p$ (mm)	$d_f$ (mm)	$l$ (mm)	$d_f/d_p$
30	0.88	2.762	0.314	1.074	0.114
30	0.95	3.285	0.286	1.181	0.087
60	0.88	1.192	0.141	0.486	0.118
60	0.95	1.491	0.124	0.541	0.083
90	0.88	0.696	0.081	0.275	0.116
90	0.95	0.772	0.064	0.299	0.083

heaters until its temperature reached the melting temperature of the tin at the top copper surface, leaving a thin tin film. The estimated tin thickness at the copper surface is 0.1 mm, which was about 2–5% of the total foam cover thickness. A clean copper foam cover was being put on the copper surface. The copper foam was welded with the copper block tightly by turning off the cartridge heaters. The thermal resistance was small between the copper surface and foam cells by the welding technique. Then the whole copper block assembly was ready for the experiment.



**Fig. 2.** Copper block test section (a) and experimental setup (b), all dimensions are in mm.

Fig. 2b shows the experimental setup and measurement systems. A transparent glass chamber containing the experimental equipments and liquid has the size of  $125 \times 127 \times 145$  mm. A stainless steel plate (3) is located at the bottom of the glass chamber. A rectangular hole was drilled at the center of the stainless steel plate to fit the copper block and the stainless steel plate by filling Teflon and epoxy glue between them for seal. The hardware arrangement ensures the copper foam exposed in the pool liquid. The part of the copper block under the plate (3) was surrounded by a glass sheath (1). As the thermal insulation material, glass fiber was filled in the gap between the copper block (2) and glass sheath (1), as shown in Fig. 2b.

A stainless steel plate (6) with a 2.0 mm thickness forms the top cover of the glass chamber. An inclined 6.0 mm diameter coiled copper tube (11) was arranged along the internal wall surface of the glass chamber. There are two holes on the plate (6) to fit the two ports of the coiled tube. The tap water is flowing in the copper tube (11) to yield a desired pool liquid temperature by adjusting the flow rate of tap water using the valve (10). In a corner of the glass chamber there is an auxiliary heater (12). The auxiliary heater (12) was turned on automatically meanwhile the valve (10) was turned off if the pool liquid temperature was below the desired value. This situation only took place at small heating power applied on the test section. For most cases it is necessary to maintain a suitable flow rate of the tap water in tube (11), with the auxiliary heater (12) turned off. The boiling induced vapor entered a reflux condenser (7). The condensed liquid returned to the glass chamber by gravity. The forced convective air dissipates heat to the environment through a fin heat sink. The condenser was vented to atmosphere by the valve (8) through a side branch tube. Thus, atmospheric pressure was always kept in the glass chamber. A K-type thermocouple (9) measures the pool liquid temperature.

The right part of Fig. 2b shows the power supply and measurement systems. The power supply system consists of a 220 V voltage stabilizer, a voltage transformer and a power meter, giving the power reading. The pool liquid temperature and three thermocouple signals were recorded by a Hewlett–Packard data acquisition system (see Fig. 2b).

Before the formal experiment, we charge liquid (water) in the glass chamber and remove the non-condensable gas in the liquid. The copper foam cover was horizontally positioned. The top liquid level was higher than the top foam cover by 100 mm. The cartridge heaters were turned on to vigorously boil the liquid for one hour to remove the non-condensable gas in foam cells and liquid. After the pool liquid reaches the environment temperature the whole system is ready for experiment. Water has good thermal performance and it is non-flammable, non-poisonous. Thus it is compatible to many kinds of material and is widely used as the working fluid. Pool boiling heat transfer experiments using water as the working fluid can be found in refs. [13–17]. An alternative liquid widely used in pool boiling heat transfer experiments is FC-72, such as reported in refs. [2,4,6,9]. Water has larger surface tension force and latent heat of evaporation than other fluids such as FC-72. The physical properties of water and vapor at atmospheric pressure are listed in Table 2.

During each experiment, we started from a small heat flux  $1\text{--}2$  W/cm<sup>2</sup> on the copper foam and specified the pool liquid temperature. The heat transfer was considered to reach a steady state if the variation of the copper block temperature was smaller than  $1^\circ\text{C}$  in ten minutes. We recorded the pool liquid temperature, the three temperatures on the copper block and the power meter reading. Then the heat flux is increased by a small step of  $2\text{--}5$  W/cm<sup>2</sup>, and the above procedure is repeated.

In the present study, the copper block below the surface immersed in the pool liquid of water was well thermally insulated.

**Table 2**  
Thermophysical properties of water and vapor at atmospheric pressure (saturation condition).

$T_{\text{sat}}$ (°C)	$\rho_f$ (kg/m <sup>3</sup> )	$\rho_g$ (kg/m <sup>3</sup> )	$C_{\text{pf}}$ (kJ/kg K)	$C_{\text{pg}}$ (kJ/kg K)	$h_{\text{fg}}$ (kJ/kg)	$\sigma$ (N/m)	$\mu_f$ (Ps.s)	$\mu_g$ (Ps.s)	$k_f$ (W/mK)
100	958.4	0.597	4.22	2.03	2257	0.0589	0.000277	0.000012	0.683

Thus one-dimensional thermal conduction heat transfer within the middle part containing  $T_1$ ,  $T_2$  and  $T_3$  (see Fig. 2a) can be assumed. Such assumption can also be found in refs. [18–20]. Based on the one-dimensional heat conduction equation, definition of the heat flux is written as  $q = -k_s \frac{dT}{dz}|_{\text{base surface}}$ , where  $k_s$  is the copper thermal conductivity,  $\frac{dT}{dz}|_{\text{base surface}}$  is the temperature gradient at the base surface,  $z$  is the coordinate perpendicular to the base surface. A least square correlation of temperatures versus  $z$  was written as  $T = a_0 + a_1 z$ , where  $a_0$ , and  $a_1$  are constants correlated based on  $T_1$ ,  $T_2$ , and  $T_3$  (see Fig. 2a). The heat flux uncertainty was estimated to be smaller than 6.0%. The surface superheat  $\Delta T_{\text{sat}}$  is defined as the surface temperature of  $T_w$  subtracting  $T_{\text{sat}}$ , where  $T_w$  is the temperature at the base surface,  $T_{\text{sat}}$  is the saturation temperature of water at atmospheric pressure. Heat transfer coefficient is calculated as

$$h = q / (T_w - T_{\text{bulk}}) \quad (1)$$

where  $T_{\text{bulk}}$  is the pool liquid temperature. The surface temperature, surface superheat, and pool liquid temperature have the maximum uncertainties of 0.3 °C. Performing the standard uncertainty analysis, we obtain the maximum relative uncertainty of  $h$  of 8.52%.

In order to evaluate the heat transfer performance enhanced by copper foams, a heat transfer enhancement ratio is defined as the heat transfer coefficient on copper foam covers divided by that on plain smooth surface, i.e.,  $En = h/h_o$ .

This study covers the following data ranges: ppi of 30, 60, 90; porosity of 0.88 and 0.95; foam cover thickness of 1.0, 2.0, 3.0, 4.0 and 5.0 mm; surface superheat from –10 to 23 K; surface heat flux up to 171 W/cm<sup>2</sup>. It is noted that the heat flux is based on the top copper surface area of 12.0 mm by 12.0 mm. The foam cell area is not involved in the computation of heat flux.

## 4. Results and discussion

### 4.1. Effect of foam ppi on the heat transfer performance

Pores per inch (ppi) strongly influences pore diameter of  $d_p$ , affecting liquid suction towards the foam covers and vapor release from the foam cells. Thus, the value of ppi has significant effect on the pool boiling heat transfer. Fig. 3 shows effect of ppi on boiling curves for various conditions. It is seen that foam covers significantly enhance heat transfer. For comparison, the wall superheats are in the range of 11–15 K at the boiling incipience on the plain smooth surface. Boiling incipience takes place at low wall superheats such as 1–4 K when foam covers are used (see Fig. 3). For the foam porosity of 0.88 shown in Fig. 3(a–b), small differences of boiling curves are identified at low wall superheats for  $\Delta T_{\text{sat}} < 10$  K, especially for the pool liquid temperature of 60 °C and foam cover thickness of 3.0 mm (see Fig. 3a). Boiling curves are identified to be different among various ppi if wall superheats are larger than 10 K, for which 60 ppi foam covers have better thermal performance than 30 and 90 ppi foam covers. For porosity of 0.95, boiling curves are different for the three foam covers of 30, 60 and 90 ppi over the whole range of wall superheats. Foam covers of 60 ppi have better thermal performance than the others.

An effective validation of the experimental results is to compare the obtained critical heat fluxes with predictions by the well known Zuber correlation [21], which is written as

$$q_{\text{CHF}} = \frac{\pi}{24} h_{\text{fg}} \rho_f^{0.5} (\sigma g (\rho_f - \rho_g))^{0.25} \quad (2)$$

The computed critical heat flux by Eq. (2) is 110 W/cm<sup>2</sup> for the saturation pool boiling heat transfer on the large plain surface with water as the working fluid. Saylor et al. [22] noted that  $q_{\text{CHF}}$  was relatively constant for large heater surfaces and increased for decreasing heater size past a certain transition point. Bar-Cohen and McNeil [23] suggested the dimensionless transition heater size as

$$L_{\text{tran}} = L(g(\rho_f - \rho_g)/\sigma)^{0.5} = 20 \quad (3)$$

where  $L$  is the transition heater size. The present heater size of 1.2 cm is sufficiently smaller than the transition heater size of 5 cm by Eq. (3). Thus the predicted critical heat flux should consider the heater size effect and be larger than the value of 110 W/cm<sup>2</sup> by Eq. (2). Rainey and You [24] recommended the experimental determined curve of  $q_{\text{CHF,small}}/q_{\text{CHF,large}}$ , which is 1.22 for the present case, where  $q_{\text{CHF,small}}$  and  $q_{\text{CHF,large}}$  are the critical heat fluxes at small heater size and large heater size, respectively. Therefore the predicted critical heat flux considering the small heater size effect is 135 W/cm<sup>2</sup>. Our measured critical heat flux is 165 W/cm<sup>2</sup> for the saturated boiling heat transfer on the smooth plain surface, which is 22% higher than the predicted value of 135 W/cm<sup>2</sup>, showing the reasonable results that we obtained. It is noted that critical heat fluxes are higher for the subcooled boiling heat transfer than those for the saturated boiling heat transfer. Critical heat flux data on the subcooled boiling heat transfer are not obtained in the present paper because temperatures at the bottom part of the copper block test section are very high. Data of critical heat flux on the subcooled boiling heat transfer are not marked in the figures in the present paper.

Enhancement of boiling heat transfer on porous surface depends on the balance between the liquid suction capability towards the porous structure, and the vapor release resistance to the pool liquid environment. Heat transfer coefficients are given in Fig. 4 for both the plain smooth surface and copper foam surfaces. Slopes of heat transfer coefficients versus heat fluxes are decreased when the heat flux  $q$  is larger than 60 W/cm<sup>2</sup> for the two porosities of 0.88 and 0.95 (see Fig. 4a and c). At high heat fluxes, boiling inside foam structures are violent. The increased vapor release resistance to the pool liquid decreases slopes of heat transfer coefficients against heat fluxes. As shown in Fig. 4a, heat transfer coefficients are suddenly decreased at the heat flux of about 60 W/cm<sup>2</sup> for the 90 ppi foam covers. The right column of Fig. 4 gives the heat transfer enhancement ratios versus heat fluxes (see Fig. 4b and d). For both the two subfigures, the heat transfer enhancement ratios are initially increased to a maximum value at low heat fluxes. Beyond the maximum point the heat transfer enhancement ratios ( $h/h_o$ ) are decreased with increases in heat fluxes. The two subfigures of Fig. 4b and d further identify that nucleate boiling is dominated by the increased nucleation sites in foam structures at low heat fluxes. But the increased vapor release resistance decreased the heat transfer enhancement ratios at larger heat

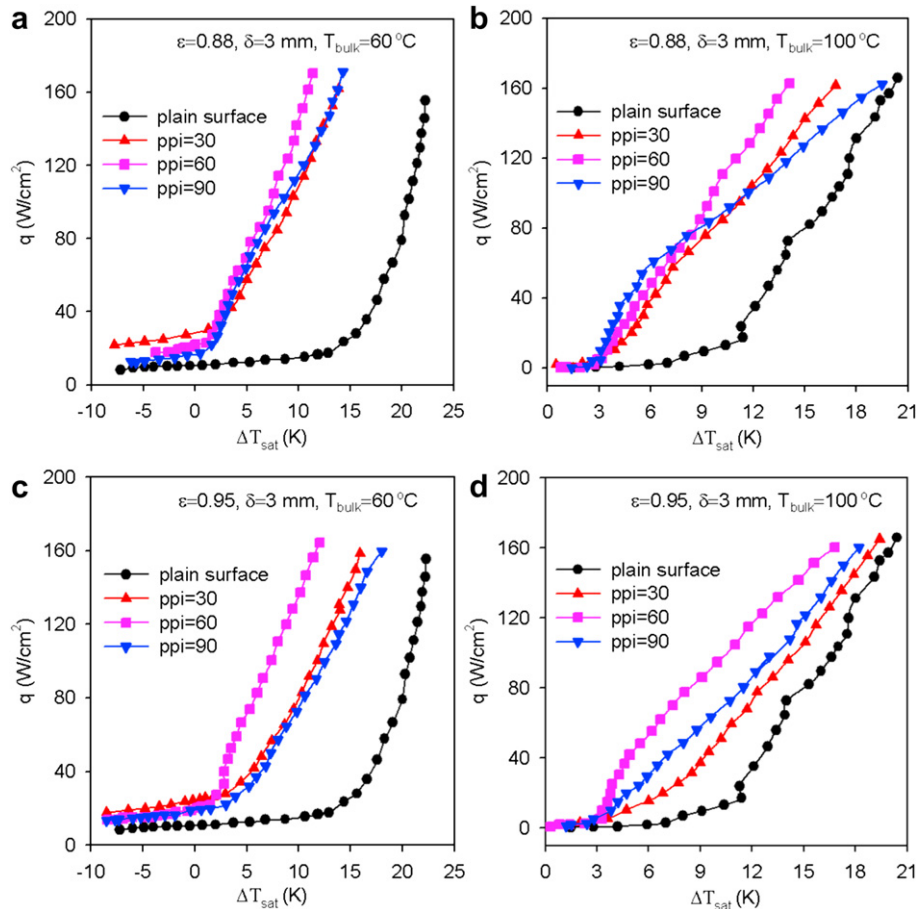


Fig. 3. Effect of ppi on boiling curves under the subcooled and saturation pool liquid conditions.

fluxes. The heat transfer coefficients are more than three times of those on the plain smooth surface maximally for the 60 ppi foam covers. For all the cases demonstrated in Fig. 4, the heat transfer enhancement ratios are larger than unity. Fig. 5 shows the heat transfer enhancement ratios versus foam ppi. Under the same conditions, heat transfer enhancement ratios display parabola distributions and attain maximum values at 60 ppi, showing great effect of foam ppi on the heat transfer performance. This phenomenon is explained as follows.

In a general sense, enhancement of pool boiling heat transfer on foam covers is attributed to the combined effect of an extended surface area, an increased nucleation site density, the resistance for vapor release from the foam cells, and a capillary-assist liquid flow towards the foam cells. The liquid supply and vapor release occur as a liquid–vapor counterflow resisting each others' motion. Meléndez and Reyes [25] gave a correlation to compute the vapor flow rate escaping from the porous coverings:

$$m = \frac{\pi}{128} \left( \frac{\rho_g \sigma}{\mu_g} \right) \left( \frac{\varepsilon d_p^3}{\delta} \right) \quad (4)$$

where  $\rho_g$  and  $\mu_g$  are the vapor density and viscosity, respectively. Eq. (4) indicates the influence of the thermal physical properties ( $\rho_g$ ,  $\sigma$ ,  $\mu_g$ ) and the porous parameters ( $\varepsilon$ ,  $d_p$ ,  $\delta$ ). A larger vapor mass flow rate represents a smaller resistance for vapor release. At the same porosity  $\varepsilon$ , low ppi foam covers have large pore size of  $d_p$ , leading to a large value of  $m$ , which is helpful for the heat transfer argument. On the other hand, low ppi foam covers have larger pore diameter of  $d_p$ , leading to the decreased capillary pumping of liquid

flow towards foam cells characterized by  $2\sigma/d_p$ . Due to the above two opposite effects of the ppi values on the pool boiling heat transfer, there is an optimal ppi value for the pool boiling heat transfer enhancement, which is 60 ppi in this paper.

#### 4.2. Effect of foam cover thickness

Foam cover thickness also significantly affects the heat transfer performance. Fig. 6 shows the boiling curves with different foam cover thicknesses. It is noted that different set of thicknesses of foam covers were used for different ppi in Fig. 6. This is because the optimal foam cover thickness is changed for different ppi. The optimal foam cover thickness is 4.0 mm for 60 ppi (see Fig. 6b) among the four thicknesses of 2.0, 3.0, 4.0 and 5.0 mm. For 30 ppi foam covers, the thickness of 2.0 mm was not tested because it will be broken when it is sliced due to the large pore diameter of 2.76 mm (see Table 1). Thus only three thicknesses of 3.0, 4.0 and 5.0 mm were tested (see Fig. 6a). The foam cover thickness of 3.0 mm provides better thermal performance among the three thicknesses of 3.0, 4.0 and 5.0 mm. For 90 ppi foam covers, the minimum thickness that we can fabricate is 1.0 mm. As shown in Fig. 6c, the thickness of 3.0 mm begins to deteriorate the heat transfer, it is not necessary to test the thickness larger than 3.0 mm. Thus the foam cover thicknesses of 1.0, 2.0 and 3.0 mm were tested. The optimal thickness is 2.0 mm for 90 ppi at relative large wall superheats such as  $\Delta T_{\text{sat}} > 8\text{K}$ . The general trend is that the optimal foam cover thickness is decreased when the ppi values are increased.

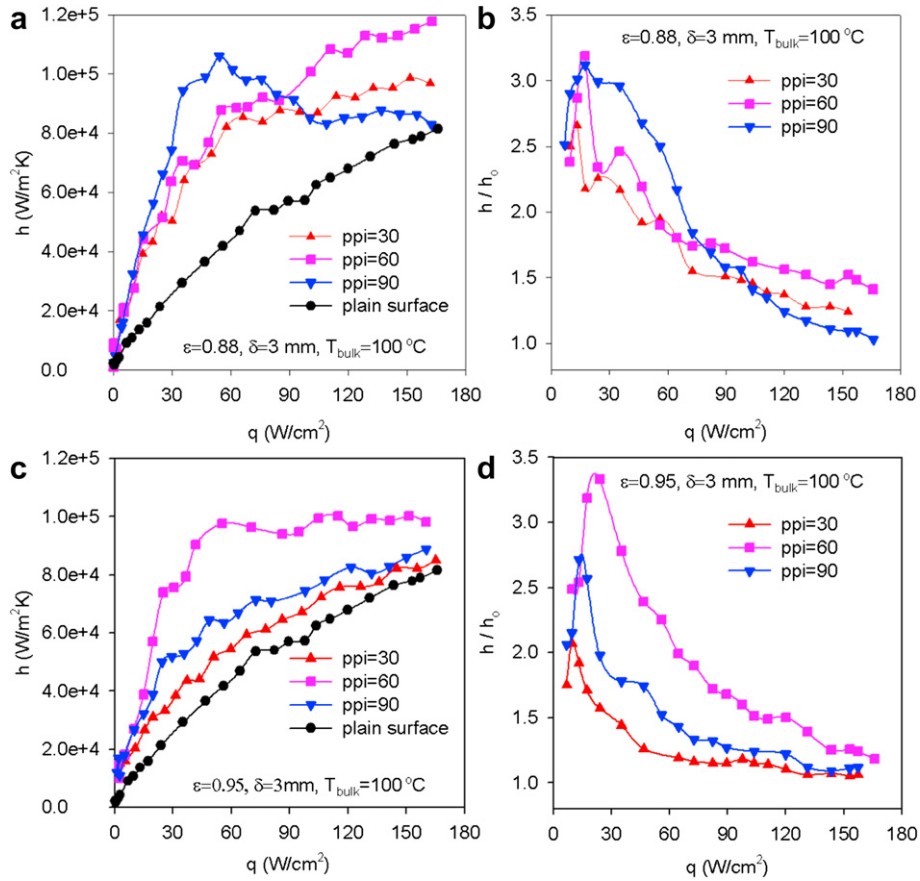


Fig. 4. Effect of ppi on heat transfer coefficients under the saturation pool liquid conditions.

Similar to the effect of foam ppi value on the nucleate boiling heat transfer, the foam cover thickness also has two opposite effects on the boiling heat transfer. Larger foam cover thickness provides more nucleation sites and extended heat transfer area, enhancing heating transfer. On the other hand, larger foam cover thickness generates larger vapor release resistance to the pool liquid, deteriorating heat transfer. Therefore, there is an optimal foam cover thickness to enhance heat transfer. Different foam ppi values have different optima foam cover thicknesses, inferring the combined effect of foam ppi value and foam cover thickness.

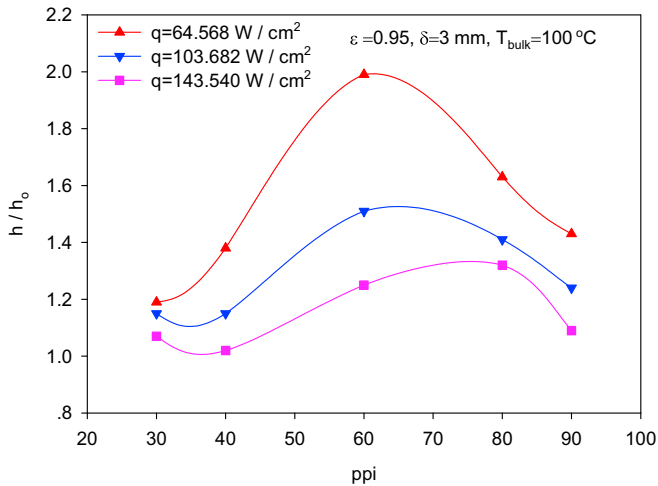


Fig. 5. Effect of ppi on the heat transfer enhancement ratio under the saturation pool liquid conditions.

Fig. 7 illustrates the boiling curves, heat transfer coefficients and heat transfer enhancement ratios. Again, a suitable foam cover thickness of 4.0 mm yields the optimal heat transfer performance among the four foam cover thicknesses of 2.0, 3.0, 4.0 and 5.0 mm for 60 ppi. Fig. 8 shows the heat transfer enhancement ratios versus the foam cover thickness. Maximum heat transfer enhancement ratios are reached at the foam cover thickness of 4.0 mm.

The available studies of heat transfer on porous media covers are mainly focused on the low porosities such as less than 0.3. Metal foams provide significantly large porosities. For the two porosities of 0.88 and 0.95 used in the present study, the heat transfer performance shows mini difference between the two porosities for most cases (see Fig. 9). However, for the saturation pool boiling heat transfer experiments, it is found that the porosity of 0.88 has slightly better thermal performance at larger wall superheats.

#### 4.3. Effect of pool liquid temperatures

Boiling curves are provided in Fig. 10 at pool liquid temperatures of 60, 80 and 100 °C on both plain surface and foam covers. For boiling heat transfer on plain surface, higher pool liquid temperatures result in larger heat flux dissipated at the same wall superheats, due to the easy generation of bubbles and agitated flow field by the bubbles at higher pool liquid temperatures. However, this trend is totally changed when foam covers are used. For all the runs tested in this paper, lower pool liquid temperatures lead to higher heat flux dissipated when other parameters are the same. Heat transfer enhancement in foam cells is caused by the combined effects of increased bubble nucleation sites, increased heat transfer area, and thermal conduction along the foam cell networks. For the

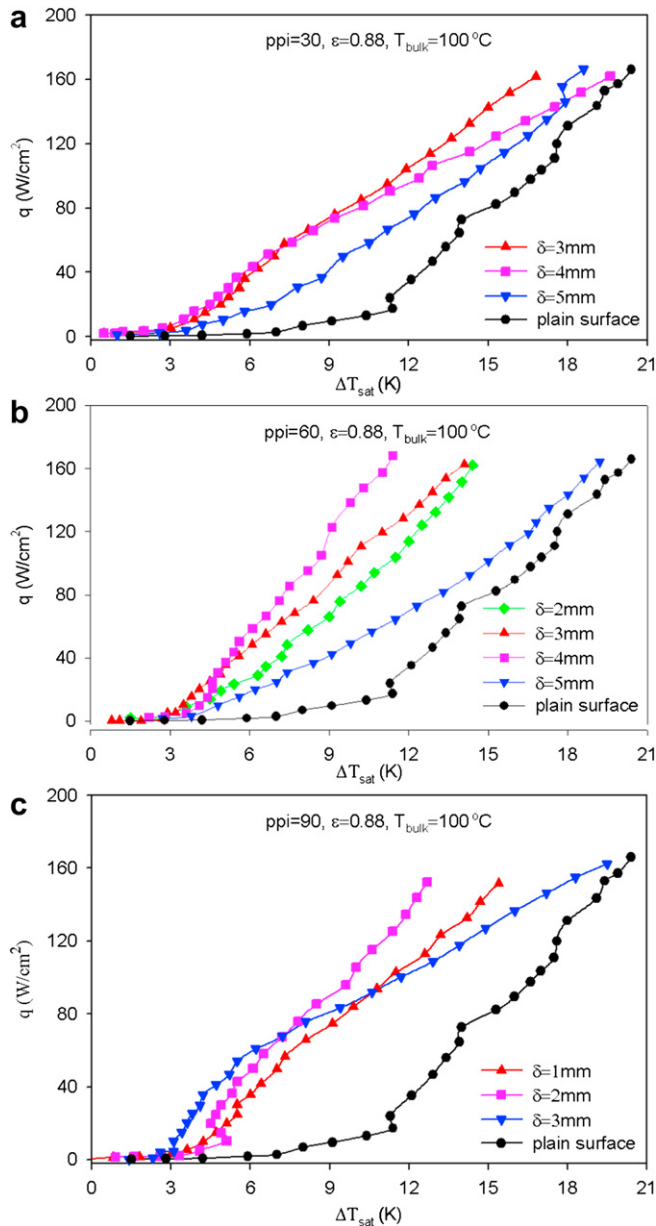


Fig. 6. Effect of foam cover thickness on boiling curves under the saturation pool liquid conditions.

90 ppi foam covers with the porosity of 0.95, effect of pool liquid temperatures on the boiling curves is not obvious. The general trend is that the effect of pool liquid temperatures becomes weak when the foam ppi value is increased.

Regarding the effect of pool liquid temperatures on the pool boiling heat transfer, there are two statements in the literature. The first statement concludes that the subcooled and saturated boiling curves almost overlap at high heat fluxes [26]. The second statement concludes that the pool liquid subcooling does influence the boiling curves and the wall superheat for the plain surface is smaller for higher bulk liquid temperature in the high heat flux region of nucleate boiling. Such phenomenon occurs in the present paper, and also appears in the literature [27–29].

Lee and Singh [27] stated that when the subcooling is introduced to pool boiling, in addition to a net increase of free convection heat transfer, the increase of subcooling produces two opposite effects on heat transfer. It increases the microconvection heat flux

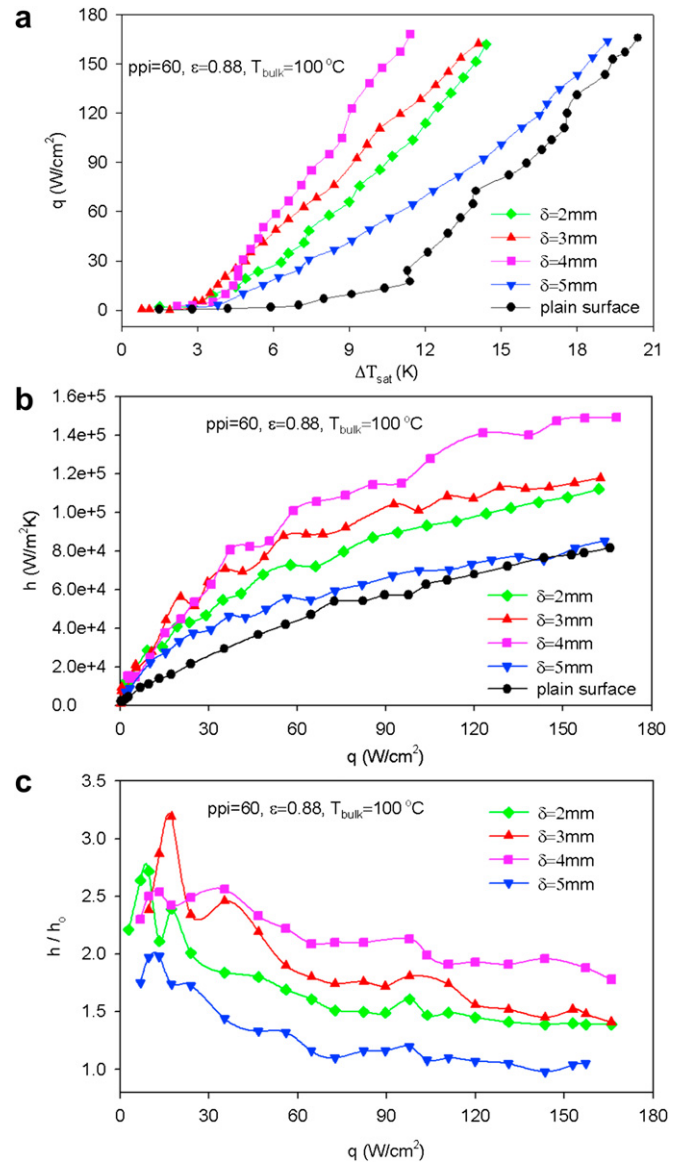
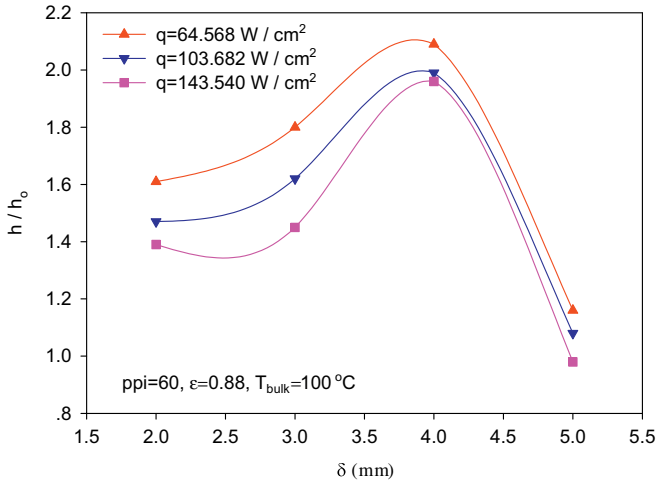


Fig. 7. Effect of foam cover thickness on the boiling curve, heat transfer coefficient, and heat transfer enhancement ratio at  $ppi=60$ ,  $\epsilon=0.88$  and  $T_{bulk}=100^\circ C$ .

due to the increase of  $\Delta T_{sat}$  and the decrease of bubble time. On the other hand, it reduces the average maximum bubble diameter, and, therefore, decreases the microconvection heat flux. The net effect of subcooling on heat transfer depends on the relative influence of these opposite effects. The nucleate boiling heat transfer is insensitive to subcooling may be explained because their conclusions were based on data in the high superheat zone. Boiling heat transfer on surfaces depends on many factors such as working fluids, surface material, roughnesses, non-condensable gas etc. Heat fluxes that can be dissipated by the pool boiling heat transfer are varied from case to case. Even though the heat flux range reported in Lee and Singh [27] is different from that in the present paper, the explanation of the two opposite effects of the liquid subcooling is reasonable and can be used to describe the subcooling effect on the pool boiling heat transfer in the present paper.

Alternatively, many studies reported that boiling curves are not overlapped for different bulk liquid temperatures [27–29]. In these studies, except for the natural convective heat transfer region, subcooling affected all test surfaces. Boiling curves were shifted to



**Fig. 8.** Effect of foam cover thickness on the heat transfer enhancement ratios at  $ppi = 60$ ,  $\epsilon = 0.88$ ,  $T_{bulk} = 100$  °C.

higher wall superheat region when bulk liquid temperatures are decreased. This means that boiling incipience was delayed by subcooling. The subcooling hinders bubble growth by condensing bubbles. Therefore, higher superheat is needed for bubble growth as the level of subcooling. Generally, the superheat increases with increasing subcooling. Judd et al. [30] suggested that this is a result of the changes in active site density, average bubble frequency, and the consequential effects on the rate of heat removal from the heater surface.

It is noted that boiling curves are only plotted for the nucleate boiling region in Kim et al. [28], i.e., there is no much data in the natural convection region. Effect of liquid subcooling on the pool boiling heat transfer reported in Kim et al. [28] supports the experimental finding reported in the present paper.

In summary, there are contrary statements on the effect of liquid subcooling on the pool boiling heat transfer. The first statement is that there is no effect of liquid subcooling on the boiling curves, such as reported in [26]. The second statement is that the liquid subcooling does affect the pool boiling heat transfer. The above contrary conclusions can be explained as follows. On the smooth plain surface on which less bubble nucleation sites are populated, boiling curves are shifting to high wall superheats when pool liquid temperatures are decreased, such as reported in the present paper and [28]. On the other hand, on the enhanced heat transfer surface

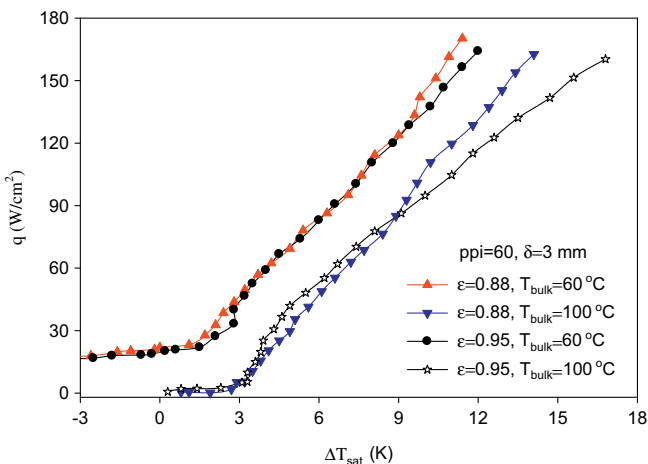


**Fig. 9.** Boiling curves of two different porosities of 0.88 and 0.95.

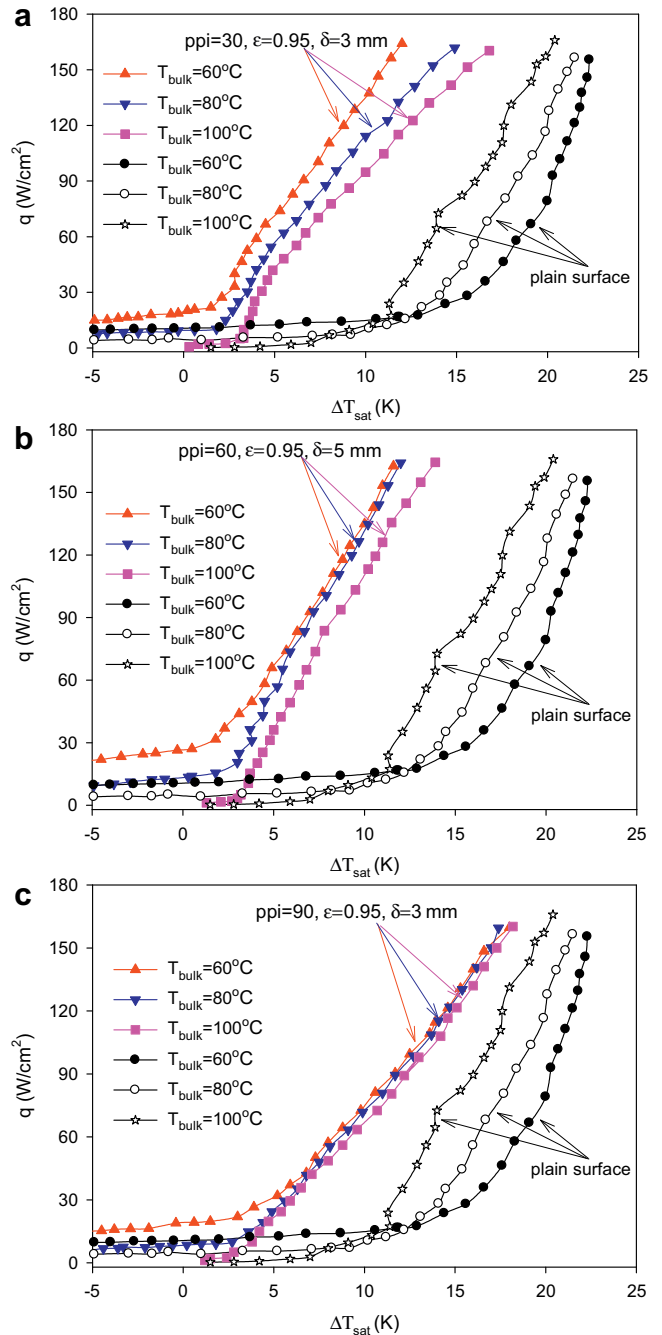


**Fig. 10.** Effect of pool liquid temperatures on boiling curves.

having sufficiently large number of bubble nucleation sites, boiling curves are shifting to low wall superheats when pool liquid temperatures are decreased, such as reported in the present paper for the boiling heat transfer on the copper foam covers and [31]. When the number of bubble nucleation sites is in a specific narrow range, boiling curves are not influenced by the pool liquid temperatures, such as reported in the text book [26].

#### 4.4. Comparison with other studies

In this paper we found that copper foams with open cells could decrease the surface superheat and eliminate the temperature excursion at boiling incipience, which is consistent with that drawn by other studies reported in Parker and El-Genk [6] for graphite

foams, Arbelaez et al. [9] and Athreya et al. [10] for metallic foam covers using FC-72 as the working fluid. Rainey and You [2] noted that pool boiling heat transfer from microporous, square pin-finned surfaces decreases the surface superheat and temperature excursion at boiling incipience. But the temperature excursion is not fully eliminated for some run cases.

In this paper degassed water was used as the working fluid, which has larger latent heat of evaporation than other fluids such as FC-72. Thus the heat transfer coefficients are much higher than those reported in the literature such as Rainey and You [2], LITER and Kaviani [3], Kim et al. [4]. The degree that the present experimental data deviate from other studies depends on the heater surface area, the parameters of enhanced microstructures used and working fluid. Honda and Wei [32] reviewed recent advances in enhancing boiling heat transfer from electronic components immersed in dielectric liquids by use of surface microstructures. The microstructures developed include surface roughnesses produced by sandblast, sputtering of SiO<sub>2</sub> layer followed by wetting etching of the surface, chemical vapor deposition of SiO<sub>2</sub> layer, laser drilled cavities, microfins, aluminum particle spraying, painting of silver flakes, or diamond particles, and heat sink studs with drilled holes, pin fins, etc. The primary issues studied are the mitigating of incipience temperature overshoot, enhancement of nucleate boiling heat transfer and increasing the critical heat flux.

The present paper identified that the foam ppi values have significant influence on the pool boiling heat transfer because the ppi value has two opposite effects on heat transfer. The optimal value is 60 ppi in the range from 30 to 90 ppi in this study. Arbelaez et al. [9] tested the foam covers in the range of 5–40 ppi with FC-72 as the working fluid. They found the increased heat transfer performance with increases of the foam ppi values, the decreased heat transfer performance with increases of foam ppi values was not observed due to the narrower range of foam ppi.

It is found that pool liquid temperatures have different effects on the pool boiling heat transfer with plain smooth surface and with foam covers. When foam covers are used boiling curves are shifted to low wall superheats with increases of pool liquid subcoolings. On the other hand, boiling curves are shifted to high wall superheats with increases of pool liquid subcoolings on plain surface, which does not support the widely accepted fact that boiling curves are overlapped each other for different subcoolings in the high heat flux region for large heater surface. But our finding of the effect of pool liquid subcooling on boiling curves at the small plain heater surface supports the similar experimental finding reported in the literature such as Lee and Singh [27], Kim et al. [28], Sathyamurthi et al. [29].

The present study uses copper foam as the heat transfer enhancement material. The pore diameter of  $d_p$  is in millimeter (see Table 1). Min et al. [8] studied 2-D and 3-D modulated porous coatings for enhanced pool boiling, focusing on the critical heat fluxes. The working fluid is PF 5060, the porous porosity is 43.8% and the particle size is in the range of 150–249  $\mu\text{m}$ , having the capability for the liquid suction towards the heater surface. Min et al. [8] found that the three heater surfaces reach a similar critical heat flux, but the slope of boiling curves is reduced as porosity increases. The critical heat flux is nearly independent of the particle diameter of the porous coatings. Generally direct comparison of the present study with Min et al. [8] is not convenient because: (1) Min et al. [8] focused on the critical heat flux while the present study mainly studies the nucleate boiling heat transfer behavior, (2) different working fluid was used, (3) different porous structures were used.

## 5. Conclusions

Pool boiling heat transfer experiments were performed using water as the working fluid. Copper foam covers were welded on the

plain surface to enhance the pool boiling heat transfer. The data range is as follows: foam ppi from 30 to 90, foam cover thickness from 1.0 to 5.0 mm, and porosity of 0.88 and 0.95. The following conclusions can be drawn:

1. Copper foam covers significantly enhance the pool boiling heat transfer. Temperatures at the Onset of Nucleate Boiling (ONB) can be decreased by 13 K maximally using copper foam structure compared with those on plain surface. Heat transfer coefficients with copper foam cells can be two to three times of those with plain surface.
2. The foam ppi has significant effect on the pool boiling heat transfer. Large ppi value with small pore size provides large number of bubble nucleation sites, but generates large resistance for vapor release. Thus there is an optimal ppi value. In the present paper the optimal ppi value is 60.
3. The combined effects of foam ppi and foam cover thickness are identified to influence the pool boiling heat transfer. Generally the optimal foam cover thickness is decreased with increase of the foam ppi values. For the 60 ppi foam cover, the optimal foam cover thickness is 4.0 mm.
4. At small foam ppi values, the heat flux that can be dissipated at the same wall superheat is decreased with increase of the pool liquid temperatures. The effect of pool liquid temperatures on the pool boiling heat transfer is weak when large foam ppi values are used.

## Acknowledgements

This paper is supported by the National Natural Science Foundation of China (50825603 and 50776089).

## References

- [1] A.E. Bergles, M.C. Chyu, Characteristics of nucleate pool boiling from porous metallic coatings. *ASME Journal of Heat Transfer* 104 (1982) 279–285.
- [2] K.N. Rainey, S.M. You, Pool boiling heat transfer from plain and microporous, square pin-finned surfaces in saturated FC-72. *Journal of Heat Transfer, ASME* 122 (2000) 509–516.
- [3] S.G. LITER, M. Kaviani, Pool boiling CHF enhancement by modulated porous-layer coating: theory and experiment. *International Journal of Heat and Mass Transfer* 44 (2001) 4287–4311.
- [4] J.H. Kim, K.N. Rainey, S.M. You, J.Y. Pak, Mechanism of nucleate boiling heat transfer enhancement from microporous surfaces in saturated FC-72. *Journal of Heat Transfer, ASME* 124 (2002) 500–506.
- [5] C.D. Ghiu, Y.K. Joshi, Visualization study of pool boiling from thin confined enhanced structures. *International Journal of Heat and Mass Transfer* 48 (2005) 4287–4299.
- [6] J.L. Parker, M.S. El-Genk, Enhanced saturation and subcooled boiling of FC-72 dielectric liquid. *International Journal of Heat and Mass Transfer* 48 (2005) 3736–3752.
- [7] G.S. Hwang, M. Kaviani, Critical heat flux in thin, uniform particle coatings. *International Journal of Heat and Mass Transfer* 49 (2006) 844–849.
- [8] D.H. Min, G.S. Hwang, Y. Usta, O.N. Cora, M. Koc, M. Kaviani, 2- and 3-D modulated coating for enhanced pool boiling. *International Journal of Heat and Mass Transfer* 52 (2009) 2607–2613.
- [9] F. Arbelaez, S. Sett, R.L. Mahajan, An experimental study on pool boiling of saturated FC-72 in highly porous aluminum metal foams, in: 34th National Heat Transfer Conference, Pittsburgh, Pennsylvania, August 20–22 (2000), pp. 759–767.
- [10] B.P. Athreya, R.L. Mahajan, S. Sett, Pool boiling of FC-72 over metal foams: effect of foam orientation and geometry, in: 8th AIAA/ASME Joint Thermophysics and Heat Transfer Conference, St. Louis, Missouri, June 24–26 (2002), pp. 1–10.
- [11] S. Moghaddam, M. Ohadi, Pool boiling of water and FC-72 on copper and graphite foams, in: Proceedings of ASME InterPACK'3, Int. Electronic Packaging Technical Conference and Exhibition, Maui, Hawaii, July 6–11 (2003), pp. 675–680.
- [12] V.V. Calmudi, Transport Phenomenon in High Porosity Metal Foams, PhD thesis, University of Colorado, CO., USA (1998).
- [13] N.K. Choon, A. Chakraborty, S.M. Aye, W. Xiaolin, New pool boiling data for water with copper-foam metal at sub-atmospheric pressures: experiments and correlation. *Applied Thermal Engineering* 26 (2006) 1286–1290.

- [14] A.K. Das, P.K. Das, P. Saha, Nucleate boiling of water from plain and structured surfaces. *Experimental Thermal and Fluid Science* 31 (2007) 967–977.
- [15] V.I. Deev, Oo Htay Lwin, V.S. Kharitonov, K.V. Kutsenko, A.A. Lavrukhin, Critical heat flux modeling in water pool boiling during power transients. *International Journal of Heat and Mass Transfer* 50 (2007) 3780–3787.
- [16] C.M. Rops, R. Lindken, J.F.M. Velthuis, J. Westerweel, Enhanced heat transfer in confined pool boiling. *International Journal of Heat and Fluid Flow* 30 (2009) 751–760.
- [17] H. Sakashita, A. Ono, Boiling behaviors and critical heat flux on a horizontal plate in saturated pool boiling of water at high pressures. *International Journal of Heat and Mass Transfer* 52 (2009) 744–750.
- [18] M.H. Shi, Y.B. Zhao, Z.L. Liu, Study on boiling heat transfer in liquid saturated particle bed and fluidized bed. *International Journal of Heat and Mass Transfer* 46 (2003) 4695–4702.
- [19] W. Wu, J.H. Du, X.J. Hu, B.X. Wang, Pool boiling heat transfer and simplified one-dimensional model for prediction on coated porous surfaces with vapor channels. *International Journal of Heat and Mass Transfer* 45 (2002) 1117–1125.
- [20] Y. Fujita, M. Tsutsui, Nucleate boiling of two and three-component mixtures. *International Journal of Heat and Mass Transfer* 47 (2004) 4637–4648.
- [21] N. Zuber, Hydrodynamic Aspects of Boiling Heat Transfer AECU-4439. *Physics and Mathematics*, US Atomic Energy Commission, 1959, 1–196.
- [22] J.R. Saylor, T.W. Simon, A. Bar-Cohen. The effect of a dimensionless length scale on the critical heat flux in saturated, pool boiling, in: R.K. Shah (Ed.), 1989 National Heat Transfer Conference, Heat Transfer Equipment Fundamentals, Design, Applications and Operating Problems, ASME HTD 108 (1989) 71–80.
- [23] A. Bar-Cohen, A. McNeil, Parametric effect of pool boiling critical heat flux in dielectric liquid. *ASME Pool and External Flow Boiling* (1992) 171–175.
- [24] K.N. Rainey, S.M. You, Effects of heater size and orientation on pool boiling heat transfer from microporous coated surfaces. *International Journal of Heat and Mass Transfer* 44 (2001) 2589–2599.
- [25] E. Meléndez, R. Reyes, The pool boiling heat transfer enhancement from experiments with binary mixtures and porous heating covers. *Experimental Thermal and Fluid Science* 30 (2006) 185–192.
- [26] S.G. Kandlikar, M. Shoji, V.K. Dhir (Eds.), *Handbook of Phase Change*, Taylor & Francis, 1999.
- [27] L. Lee, B.N. Singh, The influence of subcooling on nucleate pool boiling heat transfer. *Letters in Heat and Mass Transfer* 2 (1975) 315–324.
- [28] Y.H. Kim, K.J. Lee, D. Han, Pool boiling enhancement with surface treatments. *Heat Mass Transfer* 45 (2008) 55–60.
- [29] V. Sathyamurthi, H.S. Ahn, D. Banerjee, S.C. Lau, Subcooled pool boiling experiments on horizontal heaters coated with carbon nanotubes. *Journal of Heat Transfer, ASME* 131 (2009) 071501.1–071501.10.
- [30] R.L. Judd, H. Merte, M.E. Ulucakii, Variation of superheat with subcooling in nucleate pool boiling. *Journal of Heat Transfer, ASME* 113 (1991) 201–208.
- [31] M.S. El-Genk, J.L. Parker, Nucleate boiling of FC-72 and HFE-7100 on porous graphite at different orientations and liquid subcooling. *Energy Conversion and Management* 49 (2008) 733–750.
- [32] H. Honda, J.J. Wei, Enhancement boiling heat transfer from electronic components by use of surface microstructures. *Experimental Thermal and Fluid Science* 28 (2004) 159–169.